

## The Eta Carinae 2020 periastron passage as seen by H.E.S.S.

---

**Simon Steinmassl,<sup>a,\*</sup> Vincent Marandon,<sup>a,b</sup> Quentin Remy<sup>a</sup> and Jim Hinton<sup>a</sup> for the H.E.S.S. collaboration**

<sup>a</sup>Max-Planck-Institut für Kernphysik (MPIK), D 69029 Heidelberg, Germany

<sup>b</sup>IRFU, CEA, Université Paris-Saclay, F-91191 Gif-sur-Yvette, France

E-mail: [simon.steinmassl@mpi-hd.mpg.de](mailto:simon.steinmassl@mpi-hd.mpg.de)

The binary system Eta Carinae is a unique laboratory to study particle acceleration up to very high energies (VHE) under a wide range of conditions. Particles are thought to be accelerated at shocks forming in the wind collision region. Eta Carinae has been firmly established as a source of high energy gamma-rays in Fermi-LAT data over several orbits. With its highly eccentric orbit lasting 5.5 years, the periastron passage of the two stars is extremely close. This provides an opportunity to constrain the acceleration and absorption mechanisms of the system.

Eta Carinae was detected above 200 GeV by the H.E.S.S. telescopes (H.E.S.S. Collaboration, 2020) based on data before and after the 2014 periastron. Unfortunately the 2014 periastron itself could not be observed by H.E.S.S. due to visibility constraints. Hence the 2020 periastron was the first periastron passage visible for the full 5 telescope H.E.S.S. array and was therefore monitored with an extensive observation campaign spanning the phase range from 0.97 to 1.05.

We report the detection of a VHE signal from Eta Carinae during the 2020 periastron and describe its spectral properties together with simultaneous Fermi-LAT data. Together with previous and follow up observations, for the first time a VHE light curve spanning a full orbit is presented.

38th International Cosmic Ray Conference (ICRC2023)  
26 July - 3 August, 2023  
Nagoya, Japan



---

\*Speaker

## 1. Introduction

Situated in the Carina Nebula, the enigmatic binary system Eta Carinae ( $\eta$  Car) has been studied in detail in several wavebands over periods up to several centuries. The system, located at a distance of  $\sim 2.3$  kpc (1), consists of a luminous blue variable with a mass of  $\sim 90 M_{\odot}$  and a lighter companion with  $\sim 30 M_{\odot}$  (2).  $\eta$  Car is considered to be a colliding wind binary system in which particles are accelerated by the shocks in the wind collision region. In this region, the supersonic winds from the two stars collide to form a pair of standing shocks, separated by a contact discontinuity (3).  $\eta$  Car has been identified as a source of high energy (HE) (4) and very high energy (VHE) (5) emission by the Fermi Large Area Telescope (*Fermi*-LAT) and the High Energy Stereoscopic System (H.E.S.S.), respectively in recent years, making it unique among colliding wind binaries. The system can be tracked with current instruments over its full 5.5-year (6) orbit. The periastron passage, at which the stars are separated only on  $\sim 1$  au scales, has shown strong variability in other wavelengths, such as the X-ray regime (e.g. 7) and is hence of special importance.

The 2009, 2014 and the recent 2020 periastron passages were already followed by *Fermi*-LAT and have been discussed in several works (see e.g. 8–12). H.E.S.S. observed the 2009 periastron passage with only limited exposure yielding no detection (13). Unfortunately, the 2014 periastron passage happened outside the visibility season for H.E.S.S. allowing only for observations at phases up to 0.96 and after 1.09 for which nevertheless a significant VHE gamma-ray signal from  $\eta$  Car was reported (5). The 2020 periastron was the first periastron passage visible for H.E.S.S. in its final 5-telescope array state. Thus, a dedicated and in-depth observation campaign was planned and carried out. The results of this campaign are presented in this contribution together with data sets from previous years.

## 2. H.E.S.S. data analysis

H.E.S.S. is a 5-telescope Imaging Atmospheric Cherenkov Telescope (IACT) array situated in Namibia. It consists of 4 telescopes (CT1-4) with a mirror diameter of 12 m upgraded with new cameras in 2016 (14) and one large central 28-m telescope (CT5) with a new FlashCam prototype camera installed in 2019 (15, 16).

### 2.1 Observation campaign

The observation strategy for IACT observations of  $\eta$  Car has to be selected carefully due to the unique field of view.  $\eta$  Car lies at the heart of the Carina Nebula, which is described in optical wavelengths as a region of large-scale diffuse emission representing quite extraordinary levels of night sky background (NSB) as presented in Figure 1. To allow for stable data taking an increased trigger threshold for all five H.E.S.S. telescopes was used. For CT1-4 the trigger threshold was increased by 1 photo electron (p.e.) to 6.5 p.e., whereas for FlashCam the bright source trigger threshold of 91 p.e. per 9-pixel sum as defined in (15) was set. Furthermore, the gain of the FlashCam camera on CT5 was reduced to moonlight levels (15). Consequently, the number of switched-off pixels, even though being still considerably larger than for other observation targets, could be reduced as much as possible to less than 3 % of all pixels.

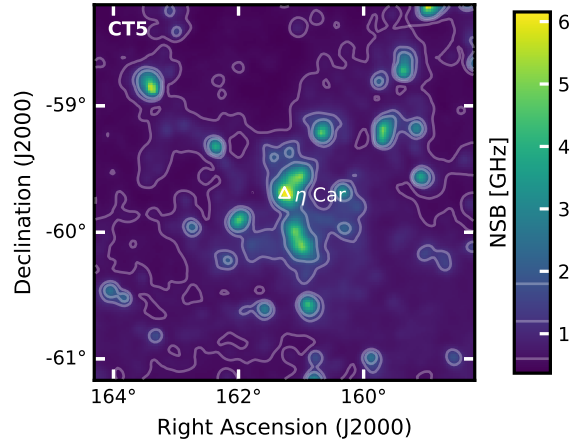


**Figure 1: Average NSB maps for the  $\eta$  Car field using CT5**

The map has been derived by averaging the NSB maps from all runs of the 2020 dataset. The position of  $\eta$  Car is shown with a white triangle. Contour levels for better visualization have been added at 0.6, 1.2 and 1.8 GHz. The map is zoomed in for better visibility of the main features.

Data set	Start Date	End Date	Live Time [h]	Mean zenith [ $^{\circ}$ ]
H.E.S.S. 1 2013-2016	Jan 13,2013	May 30,2016	20.6	39.2
H.E.S.S. 1U 2017-2019	Jan 29, 2017	Apr 7, 2019	63.3	39.2
Periastron 2020	Dec 23, 2019	May 24, 2020	97.8	39.9
"Phase 0.2" 2021	Feb 15, 2021	Apr 10, 2021	31.5	37.2

**Table 1: Basic properties of  $\eta$  Car data sets**

H.E.S.S. 1 refers to the period with the original cameras in CT1-4, whereas H.E.S.S. 1U denotes the updated CT1-4 cameras. The 2020 & 2021 datasets were taken with FlashCam installed at CT5. The live time is given for the stereo observation time and is corrected for dead time.

$\eta$  Car is visible for H.E.S.S. during the winter and spring months starting from December until the beginning of June. The observation strategy was selected to obtain as priority observations around culmination at zenith angles lower than  $40^{\circ}$  for the full observation season. During the period closely around the actual periastron passage in February 2020 a loosened zenith angle requirement with a possible extension up to  $60^{\circ}$  was considered, to maximize the exposure during this period. Unfortunately, the available observation time, especially in February, was limited due to the Namibian rainy season. Further data was acquired in spring 2021 corresponding to an orbital phase of about 0.2 assuring sufficient coverage over the entire 5.5-year orbital period together with the existing data from previous years.

After run selection, this yielded a final data set of 97.8 hours during the 2020 periastron campaign spanning a phase range from 0.97 to 1.05 and 31.5 hours in 2021. The combined observation campaigns of 2017 to 2019 had a live time of 63.3 h after selection, whereas for the 2013-16 time period 20.6 h of good-quality data was obtained. The basic properties are summarized in Table 1.

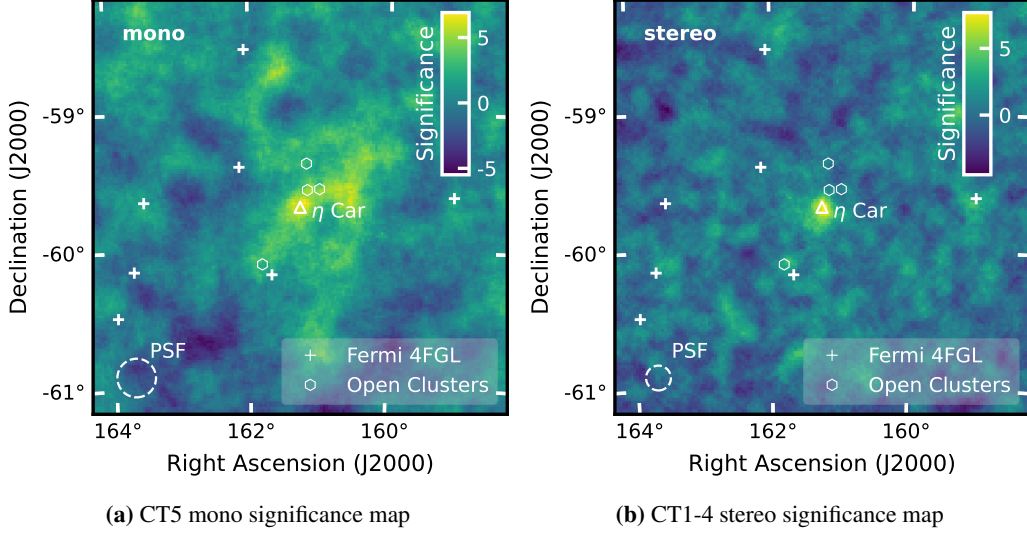


**Figure 2: Significance maps of the  $\eta$  Car periastron data set**

The resulting significance maps for CT5 mono (A) and CT1-4 stereo (B) are shown. The position of  $\eta$  Car is marked with a white triangle. Additionally, all other *Fermi*-LAT 4FGL sources (19) in the field of view are marked together with open clusters from (20).

## 2.2 CT5 mono analysis

The data from the large central telescope can be analysed in the monoscopic analysis method (17). The exceptional noise levels in the  $\eta$  Car analysis result in a mismatch when simulations that assume standard observation conditions are used. Therefore, a designated simulation set taking into account the actually measured NSB (see Figure 1) has been produced and utilized to produce custom instrument response functions valid for the  $\eta$  Car observations. To get a proper description of the background and its acceptance, test runs targeted at other sources were transformed to represent a run within the  $\eta$  Car field. These runs were then stacked and utilized through an On-Off background approach (18). The resulting significance map is shown in Figure 2a.

At the  $\eta$  Car position, a peak significance of  $7.4 \sigma$  is found. The signal appears point-like and the background normalization tested by the significance distribution is described by a Gaussian with a width of 1.3, a bit wider than the ideal case. This is taken into account as a systematic uncertainty.

A circular region with size  $\Theta = 0.13^\circ$  centered at  $\eta$  Car was chosen to derive the spectral properties. The spectral properties were modeled with a power law of the form  $\phi = \phi_0 \left(\frac{E}{E_0}\right)^{-\Gamma}$ . The lower energy threshold of the analysis is 0.14 TeV. The fit resulted in a soft spectrum with spectral index of  $\Gamma = 3.3 \pm 0.4$  and a flux normalization at a fixed reference energy  $E_0$  of 0.2 TeV of  $\phi_0 = (4.5 \pm 1.0) \times 10^{-11} \text{ TeV}^{-1} \text{ cm}^{-2} \text{ s}^{-1}$ . The systematics of the spectral parameters, especially the flux normalization, have to be treated quite conservatively. Nevertheless, even allowing for large systematic uncertainties the derived CT5 mono spectrum is inconsistent with the spectrum published in (5) based on mono data around the 2014 periastron passage. As a considerable flux reduction due to strong orbit-to-orbit variability of  $\eta$  Car seems unlikely the difference can be explained by a more advanced and careful treatment of noise factors in the analysis of the 2020 data set.

### 2.3 CT1-4 stereo analysis

For the CT1-4 stereo analysis, the ImPACT reconstruction technique (21) was chosen. As the stereo direction reconstruction is more robust against the effects of noise and the noise level is taken into account for the ImPACT-based reconstruction, no custom analysis configuration and background modeling method had to be employed. Instead, the ring background method and the reflected regions background method (18) were utilized for the derivation of maps and spectra, respectively. The results were checked using a second independent analysis chain. For the 2020 periastron data set the resulting significance map is shown in Figure 2b. At the  $\eta$  Car position a point-like signal with a significance of  $8.5 \sigma$  is found. If compared to other *Fermi*-LAT 4FGL sources (19) and known open clusters no other sources are significantly detected.

The lower energy threshold is 0.31 TeV and the reference energy was fixed at 1 TeV. Assuming again a power-law spectrum the best-fit result yielded a spectral index of  $\Gamma = 3.3 \pm 0.2$  and a flux normalization of  $\phi_0 = (2.0 \pm 0.3) \times 10^{-13} \text{ TeV}^{-1} \text{ cm}^{-2} \text{ s}^{-1}$  consistent with the mono result. The 2021 data set taken at a phase of about 0.2 was analyzed with the same methods as the 2020 data set yielding a  $5.1 \sigma$  detection and a consistent spectrum. The data sets for the years from 2013 to 2019 (see Table 1) were also analyzed with the reflected regions background method to derive a long-term light curve. Stereoscopic data sets from the years before 2012 are already published in (13).

### 3. Combined results and conclusion

In this contribution, the detection of VHE gamma-ray emission from  $\eta$  Car during its 2020 periastron is presented. Emission from  $\eta$  Car is detected over a large energy range from 0.14 TeV to above 1 TeV by the combination of data from the full H.E.S.S. array and the data covers for the first time the actual periastron passage. Together with the full H.E.S.S. data sets for the periastron passage also contemporaneous data from *Fermi*-LAT was analysed. The results of this and the resulting combined spectral energy distribution will be provided in an upcoming publication of the H.E.S.S. collaboration. This will be accompanied by a long-term light curve.

### Acknowledgments

The H.E.S.S. acknowledgments can be found at: <https://www.mpi-hd.mpg.de/hfm/HESS/pages/publications/auxiliary/HESS-Acknowledgements-2023.html>

### References

1. N. Smith, *The Astrophysical Journal* **644**, 1151, (<https://dx.doi.org/10.1086/503766>) (June 2006).
2. D. J. Hillier, K. Davidson, K. Ishibashi, T. Gull, *ApJ* **553**, 837–860 (June 2001).
3. W. Bednarek, J. Pabich, *A&A* **530**, A49, arXiv: [1104.1275](https://arxiv.org/abs/1104.1275) ([astro-ph.HE](https://arxiv.org/abs/1104.1275)) (June 2011).
4. A. A. Abdo *et al.*, *ApJ* **723**, 649–657, arXiv: [1008.3235](https://arxiv.org/abs/1008.3235) ([astro-ph.HE](https://arxiv.org/abs/1008.3235)) (Nov. 2010).

5. H.E.S.S. Collaboration *et al.*, *A&A* **635**, A167, arXiv: [2002.02336](https://arxiv.org/abs/2002.02336) ([astro-ph.HE](#)) (Mar. 2020).
6. M. Teodoro *et al.*, *ApJ* **819**, 131, arXiv: [1601.03396](https://arxiv.org/abs/1601.03396) ([astro-ph.SR](#)) (Mar. 2016).
7. A. Kashi, D. A. Principe, N. Soker, J. H. Kastner, *ApJ* **914**, 47, arXiv: [2010.03877](https://arxiv.org/abs/2010.03877) ([astro-ph.HE](#)) (June 2021).
8. K. Reitberger *et al.*, *A&A* **544**, A98, arXiv: [1203.4939](https://arxiv.org/abs/1203.4939) ([astro-ph.HE](#)) (Aug. 2012).
9. K. Reitberger, A. Reimer, O. Reimer, H. Takahashi, *A&A* **577**, A100, arXiv: [1503.07637](https://arxiv.org/abs/1503.07637) ([astro-ph.HE](#)) (May 2015).
10. M. Balbo, R. Walter, *A&A* **603**, A111, arXiv: [1705.02706](https://arxiv.org/abs/1705.02706) ([astro-ph.HE](#)) (July 2017).
11. R. White *et al.*, *A&A* **635**, A144, arXiv: [1911.01079](https://arxiv.org/abs/1911.01079) ([astro-ph.HE](#)) (Mar. 2020).
12. G. Martí-Devesa, O. Reimer, *A&A* **654**, A44, arXiv: [2109.05950](https://arxiv.org/abs/2109.05950) ([astro-ph.HE](#)) (Oct. 2021).
13. H.E.S.S. Collaboration *et al.*, *Monthly Notices of the Royal Astronomical Society* **424**, 128–135, ISSN: 0035-8711, (<https://doi.org/10.1111/j.1365-2966.2012.21180.x>) (July 2012).
14. G. Giavitto *et al.*, presented at the Proceedings of 35th International Cosmic Ray Conference — PoS(ICRC2017), vol. 301, p. 805, (<https://doi.org/10.22323/1.301.0805>).
15. B. Bi *et al.*, presented at the 37th International Cosmic Ray Conference, 743, p. 743, arXiv: [2108.03046](https://arxiv.org/abs/2108.03046) ([astro-ph.IM](#)).
16. G. Puehlhofer *et al.*, presented at the 37th International Cosmic Ray Conference. 12-23 July 2021. Berlin, 764, p. 764, (<https://doi.org/10.22323/1.395.0764>).
17. T. Murach, M. Gajdus, R. Parsons, presented at the 34th International Cosmic Ray Conference (ICRC2015), vol. 34, 1022, p. 1022.
18. D. Berge, S. Funk, J. Hinton, *A&A* **466**, 1219–1229, arXiv: [astro-ph/0610959](https://arxiv.org/abs/astro-ph/0610959) ([astro-ph](#)) (May 2007).
19. S. Abdollahi *et al.*, *ApJS* **260**, 53, arXiv: [2201.11184](https://arxiv.org/abs/2201.11184) ([astro-ph.HE](#)) (June 2022).
20. T. Preibisch *et al.*, *A&A* **530**, A34, arXiv: [1104.3477](https://arxiv.org/abs/1104.3477) ([astro-ph.GA](#)) (June 2011).
21. R. D. Parsons, J. A. Hinton, *Astroparticle Physics* **56**, 26–34, arXiv: [1403.2993](https://arxiv.org/abs/1403.2993) ([astro-ph.IM](#)) (Apr. 2014).

### Full Authors List: H.E.S.S. Collaboration

F. Aharonian<sup>1,2,3</sup>, F. Ait Benkhali<sup>4</sup>, A. Alkan<sup>5</sup>, J. Aschersleben<sup>6</sup>, H. Ashkar<sup>7</sup>, M. Backes<sup>8,9</sup>, A. Baktash<sup>10</sup>, V. Barbosa Martins<sup>11</sup>, A. Barnacka<sup>12</sup>, J. Barnard<sup>13</sup>, R. Batzofin<sup>14</sup>, Y. Becherini<sup>15,16</sup>, G. Beck<sup>17</sup>, D. Berge<sup>11,18</sup>, K. Bernlöhr<sup>2</sup>, B. Bi<sup>19</sup>, M. Böttcher<sup>9</sup>, C. Boisson<sup>20</sup>, J. Bolmont<sup>21</sup>, M. de Bony de Lavergne<sup>5</sup>, J. Borowska<sup>18</sup>, M. Bouyahiaoui<sup>2</sup>, F. Bradascio<sup>5</sup>, M. Breuhaus<sup>2</sup>, R. Brose<sup>1</sup>, A. Brown<sup>22</sup>, F. Brun<sup>5</sup>, B. Bruno<sup>23</sup>, T. Bulik<sup>24</sup>, C. Burger-Scheidlin<sup>1</sup>, T. Bylund<sup>5</sup>, F. Cangemi<sup>21</sup>, S. Caroff<sup>25</sup>, S. Casanova<sup>26</sup>, R. Cecil<sup>10</sup>, J. Celic<sup>23</sup>, M. Cerruti<sup>15</sup>, P. Chambery<sup>27</sup>, T. Chand<sup>9</sup>, S. Chandra<sup>9</sup>, A. Chen<sup>17</sup>, J. Chibueze<sup>9</sup>, O. Chibueze<sup>9</sup>, T. Collins<sup>28</sup>, G. Cotter<sup>22</sup>, P. Cristofari<sup>20</sup>, J. Damascene Mbarubucyeye<sup>11</sup>, I.D. Davids<sup>8</sup>, J. Davies<sup>22</sup>, L. de Jonge<sup>9</sup>, J. Devin<sup>29</sup>, A. Djannati-Atai<sup>15</sup>, J. Djuvsland<sup>2</sup>, A. Dmytriiev<sup>9</sup>, V. Doroshenko<sup>19</sup>, L. Dreyer<sup>9</sup>, L. Du Plessis<sup>9</sup>, K. Egberts<sup>14</sup>, S. Einecke<sup>28</sup>, J.-P. Ernenwein<sup>30</sup>, S. Fegan<sup>7</sup>, K. Feijen<sup>15</sup>, G. Fichet de Clairfontaine<sup>20</sup>, G. Fontaine<sup>7</sup>, F. Lott<sup>8</sup>, M. Fülling<sup>11</sup>, S. Funk<sup>23</sup>, S. Gabici<sup>15</sup>, Y.A. Gallant<sup>29</sup>, S. Ghafourizadeh<sup>4</sup>, G. Giavitto<sup>11</sup>, L. Giunti<sup>15,5</sup>, D. Glawion<sup>23</sup>, J.F. Glicenstein<sup>5</sup>, J. Glombitza<sup>23</sup>, P. Goswami<sup>15</sup>, G. Grolleron<sup>21</sup>, M.-H. Grondin<sup>27</sup>,

L. Haerer<sup>2</sup>, S. Hattingh<sup>9</sup>, M. Haupt<sup>11</sup>, G. Hermann<sup>2</sup>, J.A. Hinton<sup>2</sup>, W. Hofmann<sup>2</sup>, T. L. Holch<sup>11</sup>, M. Holler<sup>31</sup>, D. Horns<sup>10</sup>, Zhiqiu Huang<sup>2</sup>, A. Jaitly<sup>11</sup>, M. Jamroz<sup>12</sup>, F. Jankowsky<sup>4</sup>, A. Jardin-Blicq<sup>27</sup>, V. Joshi<sup>23</sup>, I. Jung-Richardt<sup>23</sup>, E. Kasai<sup>8</sup>, K. Katarzyński<sup>32</sup>, H. Katjaita<sup>8</sup>, D. Khangulyan<sup>33</sup>, R. Khatoon<sup>9</sup>, B. Khélifi<sup>15</sup>, S. Klepser<sup>11</sup>, W. Kluźniak<sup>34</sup>, Nu. Komin<sup>17</sup>, R. Konno<sup>11</sup>, K. Kosack<sup>5</sup>, D. Kostunin<sup>11</sup>, A. Kundu<sup>9</sup>, G. Lamanna<sup>25</sup>, R.G. Lang<sup>23</sup>, S. Le Stum<sup>30</sup>, V. Lefranc<sup>5</sup>, F. Leitl<sup>23</sup>, A. Lemièrè<sup>15</sup>, M. Lemoine-Goumard<sup>27</sup>, J.-P. Lenain<sup>21</sup>, F. Leuschner<sup>19</sup>, A. Luashvili<sup>20</sup>, I. Lypova<sup>4</sup>, J. Mackey<sup>1</sup>, D. Malyshev<sup>19</sup>, D. Malyshev<sup>23</sup>, V. Marandon<sup>5</sup>, A. Marcowith<sup>29</sup>, P. Marinos<sup>28</sup>, G. Martí-Devesa<sup>31</sup>, R. Marx<sup>4</sup>, G. Maurin<sup>25</sup>, A. Mehta<sup>11</sup>, P.J. Meintjes<sup>13</sup>, M. Meyer<sup>10</sup>, A. Mitchell<sup>23</sup>, R. Moderski<sup>34</sup>, L. Mohrmann<sup>2</sup>, A. Montanari<sup>4</sup>, C. Moore<sup>35</sup>, E. Moulin<sup>5</sup>, T. Murach<sup>11</sup>, K. Nakashima<sup>23</sup>, M. de Naurois<sup>7</sup>, H. Ndiyavala<sup>8,9</sup>, J. Niemiec<sup>26</sup>, A. Priyana Noel<sup>12</sup>, P. O'Brien<sup>35</sup>, S. Ohm<sup>11</sup>, L. Olivera-Nieto<sup>2</sup>, E. de Ona Wilhelmi<sup>11</sup>, M. Ostrowski<sup>12</sup>, E. Oukacha<sup>15</sup>, S. Panny<sup>31</sup>, M. Panter<sup>2</sup>, R.D. Parsons<sup>18</sup>, U. Pensec<sup>21</sup>, G. Peron<sup>15</sup>, S. Pita<sup>15</sup>, V. Poireau<sup>25</sup>, D.A. Prokhorov<sup>36</sup>, H. Prokoph<sup>11</sup>, G. Pühlhofer<sup>19</sup>, M. Punch<sup>15</sup>, A. Quirrenbach<sup>4</sup>, M. Regeard<sup>15</sup>, P. Reichherzer<sup>5</sup>, A. Reimer<sup>31</sup>, O. Reimer<sup>31</sup>, I. Reis<sup>5</sup>, Q. Remy<sup>2</sup>, H. Ren<sup>2</sup>, M. Renaud<sup>29</sup>, B. Reville<sup>2</sup>, F. Rieger<sup>2</sup>, G. Roellinghoff<sup>23</sup>, E. Rol<sup>36</sup>, G. Rowell<sup>28</sup>, B. Rudak<sup>34</sup>, H. Rueda Ricarte<sup>5</sup>, E. Ruiz-Velasco<sup>2</sup>, K. Sabri<sup>29</sup>, V. Sahakian<sup>37</sup>, S. Sailer<sup>2</sup>, H. Salzmann<sup>19</sup>, D.A. Sanchez<sup>25</sup>, A. Santangelo<sup>19</sup>, M. Sasaki<sup>23</sup>, J. Schäfer<sup>23</sup>, F. Schüssler<sup>5</sup>, H.M. Schutte<sup>9</sup>, M. Senniappan<sup>16</sup>, J.N.S. Shapopi<sup>8</sup>, S. Shilunga<sup>8</sup>, K. Shiningayamwe<sup>8</sup>, H. Sol<sup>20</sup>, H. Spackman<sup>22</sup>, A. Specovius<sup>23</sup>, S. Spencer<sup>23</sup>, E. Stawarz<sup>12</sup>, R. Steenkamp<sup>8</sup>, C. Stegmann<sup>14,11</sup>, S. Steinmassl<sup>2</sup>, C. Steppa<sup>14</sup>, K. Streil<sup>23</sup>, I. Sushch<sup>9</sup>, H. Suzuki<sup>38</sup>, T. Takahashi<sup>39</sup>, T. Tanaka<sup>38</sup>, T. Tavernier<sup>5</sup>, A.M. Taylor<sup>11</sup>, R. Terrier<sup>15</sup>, A. Thakur<sup>28</sup>, J. H.E. Thiersen<sup>9</sup>, C. Thorpe-Morgan<sup>19</sup>, M. Tluczykont<sup>10</sup>, M. Tsirou<sup>11</sup>, N. Tsuji<sup>40</sup>, R. Tuffs<sup>2</sup>, Y. Uchiyama<sup>33</sup>, M. Ullmo<sup>5</sup>, T. Unbehaun<sup>23</sup>, P. van der Merwe<sup>9</sup>, C. van Eldik<sup>23</sup>, B. van Soelen<sup>13</sup>, G. Vasileiadis<sup>29</sup>, M. Vecchi<sup>6</sup>, J. Veh<sup>23</sup>, C. Venter<sup>9</sup>, J. Vink<sup>36</sup>, H.J. Völk<sup>2</sup>, N. Vogel<sup>23</sup>, T. Wach<sup>23</sup>, S.J. Wagner<sup>4</sup>, F. Werner<sup>2</sup>, R. White<sup>2</sup>, A. Wiercholska<sup>26</sup>, Yu Wun Wong<sup>23</sup>, H. Yassin<sup>9</sup>, M. Zacharias<sup>4,9</sup>, D. Zargaryan<sup>1</sup>, A.A. Zdziarski<sup>34</sup>, A. Zech<sup>20</sup>, S.J. Zhu<sup>11</sup>, A. Zmija<sup>23</sup>, S. Zouari<sup>15</sup> and N. Żywucka<sup>9</sup>.

<sup>1</sup>Dublin Institute for Advanced Studies, 31 Fitzwilliam Place, Dublin 2, Ireland

<sup>2</sup>Max-Planck-Institut für Kernphysik, P.O. Box 103980, D 69029 Heidelberg, Germany

<sup>3</sup>Yerevan State University, 1 Alek Manukyan St, Yerevan 0025, Armenia

<sup>4</sup>Landessternwarte, Universität Heidelberg, Königstuhl, D 69117 Heidelberg, Germany

<sup>5</sup>IRFU, CEA, Université Paris-Saclay, F-91191 Gif-sur-Yvette, France

<sup>6</sup>Kapteyn Astronomical Institute, University of Groningen, Landleven 12, 9747 AD Groningen, The Netherlands

<sup>7</sup>Laboratoire Leprince-Ringuet, École Polytechnique, CNRS, Institut Polytechnique de Paris, F-91128 Palaiseau, France

<sup>8</sup>University of Namibia, Department of Physics, Private Bag 13301, Windhoek 10005, Namibia

<sup>9</sup>Centre for Space Research, North-West University, Potchefstroom 2520, South Africa

<sup>10</sup>Universität Hamburg, Institut für Experimentalphysik, Luruper Chaussee 149, D 22761 Hamburg, Germany

<sup>11</sup>Deutsches Elektronen-Synchrotron DESY, Platanenallee 6, 15738 Zeuthen, Germany

<sup>12</sup>Obserwatorium Astronomiczne, Uniwersytet Jagielloński, ul. Orła 171, 30-244 Kraków, Poland

<sup>13</sup>Department of Physics, University of the Free State, PO Box 339, Bloemfontein 9300, South Africa

<sup>14</sup>Institut für Physik und Astronomie, Universität Potsdam, Karl-Liebknecht-Strasse 24/25, D 14476 Potsdam, Germany

<sup>15</sup>Université de Paris, CNRS, Astroparticule et Cosmologie, F-75013 Paris, France

<sup>16</sup>Department of Physics and Electrical Engineering, Linnaeus University, 351 95 Växjö, Sweden

<sup>17</sup>School of Physics, University of the Witwatersrand, 1 Jan Smuts Avenue, Braamfontein, Johannesburg, 2050 South Africa

<sup>18</sup>Institut für Physik, Humboldt-Universität zu Berlin, Newtonstr. 15, D 12489 Berlin, Germany

<sup>19</sup>Institut für Astronomie und Astrophysik, Universität Tübingen, Sand 1, D 72076 Tübingen, Germany

<sup>20</sup>Laboratoire Univers et Théories, Observatoire de Paris, Université PSL, CNRS, Université Paris Cité, 5 Pl. Jules Janssen, 92190 Meudon, France

<sup>21</sup>Sorbonne Université, Université Paris Diderot, Sorbonne Paris Cité, CNRS/IN2P3, Laboratoire de Physique Nucléaire et de Hautes Energies, LPNHE, 4 Place Jussieu, F-75252 Paris, France

<sup>22</sup>University of Oxford, Department of Physics, Denys Wilkinson Building, Keble Road, Oxford OX1 3RH, UK

<sup>23</sup>Friedrich-Alexander-Universität Erlangen-Nürnberg, Erlangen Centre for Astroparticle Physics, Nikolaus-Fiebiger-Str. 2, 91058 Erlangen, Germany

<sup>24</sup>Astronomical Observatory, The University of Warsaw, Al. Ujazdowskie 4, 00-478 Warsaw, Poland

<sup>25</sup>Université Savoie Mont Blanc, CNRS, Laboratoire d'Annecy de Physique des Particules - IN2P3, 74000 Annecy, France

<sup>26</sup>Instytut Fizyki Jądrowej PAN, ul. Radzikowskiego 152, 31-342 Kraków, Poland

<sup>27</sup>Université Bordeaux, CNRS, LP2I Bordeaux, UMR 5797, F-33170 Gradignan, France

<sup>28</sup>School of Physical Sciences, University of Adelaide, Adelaide 5005, Australia

<sup>29</sup>Laboratoire Univers et Particules de Montpellier, Université Montpellier, CNRS/IN2P3, CC 72, Place Eugène Bataillon, F-34095 Montpellier Cedex 5, France

<sup>30</sup>Aix Marseille Université, CNRS/IN2P3, CPPM, Marseille, France

<sup>31</sup>Universität Innsbruck, Institut für Astro- und Teilchenphysik, Technikerstraße 25, 6020 Innsbruck, Austria

<sup>32</sup>Institute of Astronomy, Faculty of Physics, Astronomy and Informatics, Nicolaus Copernicus University, Grudziadzka 5, 87-100 Torun, Poland

<sup>33</sup>Department of Physics, Rikkyo University, 3-34-1 Nishi-Ikebukuro, Toshima-ku, Tokyo 171-8501, Japan

<sup>34</sup>Nicolaus Copernicus Astronomical Center, Polish Academy of Sciences, ul. Bartycka 18, 00-716 Warsaw, Poland

<sup>35</sup>Department of Physics and Astronomy, The University of Leicester, University Road, Leicester, LE1 7RH, United Kingdom

<sup>36</sup>GRAPPA, Anton Pannekoek Institute for Astronomy, University of Amsterdam, Science Park 904, 1098 XH Amsterdam, The Netherlands



lands

<sup>37</sup>Yerevan Physics Institute, 2 Alikhanian Brothers St., 0036 Yerevan, Armenia

<sup>38</sup>Department of Physics, Konan University, 8-9-1 Okamoto, Higashinada, Kobe, Hyogo 658-8501, Japan

<sup>39</sup>Kavli Institute for the Physics and Mathematics of the Universe (WPI), The University of Tokyo Institutes for Advanced Study (UTIAS), The University of Tokyo, 5-1-5 Kashiwa-no-Ha, Kashiwa, Chiba, 277-8583, Japan

<sup>40</sup>RIKEN, 2-1 Hirosawa, Wako, Saitama 351-0198, Japan